

Magnetic field control of topological magnon-polaron bands in two-dimensional ferromagnets

Pengtao Shen and Se Kwon Kim

Department of Physics and Astronomy, University of Missouri, Columbia, Missouri 65211, USA

(Dated: October 22, 2019)

We theoretically study magnon-phonon hybrid excitations in a square lattice ferromagnet subjected to a magnetic field by varying the field direction. The bulk bands of hybrid excitations, which are referred to as magnon-polarons, are investigated by considering all three phonon modes: vertical phonon, transverse phonon, and longitudinal phonon. We show that the topological properties of three hybridizations are different in terms of the Berry curvature and the Chern numbers. We also find that the topological properties of the bands can be controlled by changing the direction of the magnetic field, exhibiting one or more topological phase transitions. The dependence of thermal Hall conductivity as a function of magnetic field direction is proposed as an experiment probe of our theoretical results.

I. INTRODUCTION

Since the discovery of the quantum Hall effects [1–3], intrinsic topological properties of electronic bands have been a subject of long standing interest. The Berry phase and Berry curvature [4] of electron bands, which characterize their topological properties, are responsible for various electron transport phenomena such as the anomalous Hall effect [5, 6] and the spin Hall effect [7–9]. The study of the Berry curvature has been extended to collective bosonic excitations such as magnons [10–14] and phonons [15–17]. The finite Berry curvature of the bosonic bands can also give rise to various Hall effects such as the thermal Hall effect [10–14, 17]. Besides these, the hybridized excitation of magnons and phonons, which is called magnetoelastic wave [18] or magnon-polaron [19], has also been predicted to exhibit a finite Berry curvature and possess the associated nontrivial topology, e.g., in ferromagnets with long-range dipolar interaction [20] or Dzyaloshinskii-Moriya (DM) interaction [21], in noncollinear antiferromagnets with exchange magnetorestriction [22], and in collinear ferrimagnets with DM-induced magnon-phonon coupling [23].

Even without such long-range dipolar interaction, DM interaction, or special lattice symmetry, recent works [24, 25] have shown that the nontrivial topology of magnon-polaron can emerge in a two-dimensional (2D) magnet by taking account of the well-known magnetoelastic interaction driven by Kittel [26]. In particular, it has been shown that the topological structure can be controlled by the magnetic field via the change of the number of band-crossing lines. However, the previous investigations have been restricted to the cases where the magnetic field and the ground-state spin direction are perpendicular to the plane, and, in that case, magnons only couple with out-of-plane (ZA) phonons, not affecting the other in-plane phonon modes.

In this paper, we study a more general problem: topological properties of magnon-phonon modes in a square lattice ferromagnet subjected to a magnetic field in an arbitrary direction. See Fig. 1 for the schematic illus-

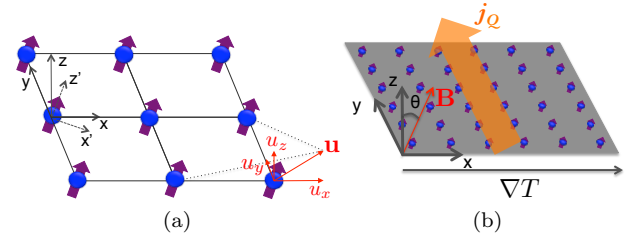


FIG. 1: (a) The schematic illustration of the model system, where spins denoted by arrows are arranged in a square lattice. The external magnetic field \mathbf{B} is in x - z plane with tilt angle θ from the z axis. The ground state is given by the uniform spin state along the magnetic field \mathbf{B} . x' - y' - z' is the rotated coordinate frame, where z' is the spin direction in the ground state. The displacement vector of ions is denoted by the three-dimensional vector $\mathbf{u} = (u_x, u_y, u_z)$. (b) The schematic illustration of the thermal Hall effect, which refers to the generation of the transverse heat flux \mathbf{j}_Q by a temperature gradient ∇T in the longitudinal direction. In our work, the thermal Hall effect is induced by the finite Berry curvature of magnon-polarons.

tration of the system. When the magnetic field is away from z direction, the magnons couples not only with ZA phonons, but also with in-plane phonons. Since there are two types of in-plane phonons, longitudinal (LA) phonon and transverse (TA) phonon [27–30] in 2D thin film, the dependence of the topological property as well as the thermal Hall conductivity on the field direction are investigated by considering all three phonon modes: vertical, transverse, and longitudinal phonons. Specifically, we investigate the topological structures of the magnon-polaron bands by mapping our model to the well-known two-band model of topological insulator [9] by focusing on each band crossing lines. As an experimental probe, we propose the dependence of thermal Hall conductivity on the magnetic field direction.

Our paper is organized as follows. In Sec. II, we de-

scribe our model including magnetic interaction, elastic interaction and magnetoelastic coupling. In Sec. III, we study the effect of magnon-phonon coupling on the collective excitations and their topological structures. In Sec IV, we present our results on experimental prediction of the thermal Hall conductivity as a function of magnetic field direction. We conclude the paper in Sec. V by providing summary and outlook.

II. MODEL

Our model system is a 2D ferromagnet on a square lattice described by the Hamiltonian

$$H = H_{\text{mag}} + H_{\text{ph}} + H_{\text{mp}}, \quad (1)$$

where H_{mag} and H_{ph} are the magnetic and elastic subsystem, respectively, and H_{mp} is the magnetoelastic term between them. We will describe each term in detail below.

A. Magnetic Subsystem

The magnetic term is given by

$$H_{\text{mag}} = -J \sum_{i,j} \mathbf{S}_i \cdot \mathbf{S}_j - \mathbf{B} \cdot \sum_i \mathbf{S}_i \quad (2)$$

where $J > 0$ is the ferromagnetic Heisenberg exchange interaction and $\mathbf{B} = B(\sin \theta, 0, \cos \theta)$ is the external magnetic field with a tilt angle θ from z axis rotated about y axis. The ground state of spin direction is along \mathbf{B} , $\mathbf{n}_0 = (\sin \theta, 0, \cos \theta)$.

To obtain the magnon band, we will work in a rotated spin frame, where z' is in the direction of \mathbf{B} , y' is the same as y and x' is chosen according to right-handed coordinate system. We perform Holstein-Primakoff transformation, $S_i^{x'} \approx (\sqrt{2S}/2)(a_i + a_i^\dagger)$, $S_i^{y'} \approx (\sqrt{2S}/2)(a_i - a_i^\dagger)$, $S_i^{z'} = S - a_i^\dagger a_i$, where a_i and a_i^\dagger are, respectively, the annihilation and the creation operators of a magnon at site i. By taking the Fourier transformation, $a_i = \sum_{\mathbf{k}} e^{i\mathbf{k} \cdot \mathbf{R}_i} a_{\mathbf{k}}/N$, where N is the number of sites in the system, we diagonalize the magnetic Hamiltonian in the momentum space:

$$H_{\text{mag}} = \sum_{\mathbf{k}} \hbar \omega_{\text{m}}(\mathbf{k}) a_{\mathbf{k}}^\dagger a_{\mathbf{k}}, \quad (3)$$

where the magnon dispersion is given by $\omega_{\text{m}}(\mathbf{k}) = [2JS(2 - \cos k_x - \cos k_y) + B]/\hbar$. Here and thereafter, we set lattice constant $a = 1$. In long wavelength limit, we obtain the dispersion

$$\omega_{\text{m}}(\mathbf{k}) = (JSk^2 + B)/\hbar. \quad (4)$$

The magnon dispersion is quadratic at small wavevector with a gap $\propto B$.

B. Elastic Subsystem

The phonon system accounting for the elastic degree of freedom of the lattice is described by the following Hamiltonian:

$$H_{\text{ph}} = \sum_i \frac{\mathbf{p}_i^2}{2M} + \frac{1}{2} \sum_{i,j,\alpha,\beta} u_i^\alpha \Phi_{i,j}^{\alpha,\beta} u_j^\beta, \quad (5)$$

where \mathbf{u}_i is the displacement vector of the i th ion from its equilibrium position, \mathbf{p}_i is the conjugate momentum vector, M is the ion mass, and $\Phi_{i,j}^{\alpha,\beta}$ is a force constant matrix between site i and site j ($\alpha, \beta = x, y, z$). We consider a lattice model with in-plane force constant between nearest and second nearest neighbor to be a_1 and a_2 , and out-of-plane force constant between nearest neighbor to be a_3 . It is convenient to describe in the momentum space,

$$\begin{aligned} H_{\text{ph}}^{xy} &= \sum_{\mathbf{k}} \frac{p_{-\mathbf{k}}^\alpha p_{\mathbf{k}}^\alpha}{2M} + \frac{1}{2} u_{-\mathbf{k}}^\alpha \Phi^{\alpha\beta}(\mathbf{k}) u_{\mathbf{k}}^\beta, \\ H_{\text{ph}}^z &= \sum_{\mathbf{k}} \frac{p_{-\mathbf{k}}^z p_{\mathbf{k}}^z}{2M} + \frac{1}{2} u_{-\mathbf{k}}^z \Phi^z(\mathbf{k}) u_{\mathbf{k}}^z, \end{aligned} \quad (6)$$

where $\Phi^{xx}(\mathbf{k}) = 2a_1(1 - \cos k_x) + 2a_2(1 - \cos k_x \cos k_y)$, $\Phi^{xy}(\mathbf{k}) = 2a_2 \sin k_x \sin k_y$, $\Phi^{yx}(\mathbf{k}) = 2a_2 \sin k_x \sin k_y$, $\Phi^{yy}(\mathbf{k}) = 2a_1(1 - \cos k_y) + 2a_2(1 - \cos k_x \cos k_y)$ and $\Phi^z(\mathbf{k}) = 2a_3(2 - \cos k_x - \cos k_y)$. Note that in-plane and out-of-plane mode do not couple [28–30], as $u^x u^z$ and $u^y u^z$ terms must vanish under the mirror symmetry for 2D system.

We can obtain diagonalized phonon Hamiltonian in quantized phonon operators, $b_{\mathbf{k},i}$ and $b_{\mathbf{k},i}^\dagger$, for longitudinal acoustic(LA) mode, in-plane transverse acoustic(TA) mode from first equation, for out-of-plane transverse acoustic(ZA) mode from second equation.

$$H_{\text{ph}} = \sum_{\mathbf{k}} \hbar \omega_{\text{p}}^i(\mathbf{k}) (b_{\mathbf{k},i}^\dagger b_{\mathbf{k},i} + \frac{1}{2}), \quad (7)$$

where $\omega_{\text{p}}^L(\mathbf{k})$, $\omega_{\text{p}}^T(\mathbf{k})$, $\omega_{\text{p}}^Z(\mathbf{k})$ are phonon dispersions for LA, TA and ZA phonon mode, respectively. $\omega_{\text{p}}^Z(\mathbf{k}) = \sqrt{\Phi^z(\mathbf{k})/M}$ and $\omega_{\text{p}}^{L/T}(\mathbf{k}) = \sqrt{\Phi^{L/T}(\mathbf{k})/M}$, where $\Phi^{L/T}(\mathbf{k})$ are two eigenvalues of $\Phi^{\alpha\beta}(\mathbf{k})$. In the long wavelength limit,

$$\begin{aligned} \omega_{\text{p}}^Z(\mathbf{k}) &= v_{\text{p}}^Z k, \\ \omega_{\text{p}}^L(\mathbf{k}) &= v_{\text{p}}^L(\phi_k) k, \\ \omega_{\text{p}}^T(\mathbf{k}) &= v_{\text{p}}^T(\phi_k) k, \end{aligned} \quad (8)$$

where phonon velocities are $v_{\text{p}}^Z = \sqrt{a_3/M}$ and $v_{\text{p}}^{L/T}(\phi_k) = [(a_1 + 2a_2 \pm \sqrt{\cos^2 2\phi_k a_1^2 + 4 \sin^2 2\phi_k a_2^2})/2M]^{1/2}$, where $+/-$ are chosen for LA/TA respectively. It can be easily found from above equation that phonon velocity of LA phonon is larger than TA phonon. We will consider thin film, where less strain is in out-of plane

direction than in-plane direction, and therefore we will assume $v_p^L > v_p^T > v_p^Z$ [28–30].

The phonon operators are introduced in such a way that

$$\begin{aligned} u_{\mathbf{k}}^Z &= \frac{1}{2} \sqrt{\frac{\hbar}{M\omega_p^Z(\mathbf{k})}} \left(\frac{b_{\mathbf{k},Z} + b_{-\mathbf{k},Z}^\dagger}{\sqrt{2}} \right), \\ p_{\mathbf{k}}^Z &= \sqrt{\hbar M\omega_p^Z(\mathbf{k})} \left(\frac{b_{-\mathbf{k},Z} - b_{\mathbf{k},Z}^\dagger}{\sqrt{2}i} \right), \end{aligned} \quad (9)$$

and for in plane vibration,

$$\begin{aligned} \mathbf{u}_{\mathbf{k}}^{L/T} &= \sqrt{\frac{\hbar}{M\omega_p^{L/T}(\mathbf{k})}} \left(\frac{b_{\mathbf{k},L/T} + b_{-\mathbf{k},L/T}^\dagger}{\sqrt{2}} \right) \hat{\mathbf{e}}^{L/T}(\mathbf{k}), \\ \mathbf{p}_{\mathbf{k}}^{L/T} &= \sqrt{\hbar M\omega_p^{L/T}(\mathbf{k})} \left(\frac{b_{-\mathbf{k},L/T} - b_{\mathbf{k},L/T}^\dagger}{\sqrt{2}i} \right) \hat{\mathbf{e}}^{L/T}(\mathbf{k}), \end{aligned} \quad (10)$$

where $\hat{\mathbf{e}}^{L/T}(\mathbf{k})$ are the normalized two-dimensional eigenvectors of $\Phi^{\alpha\beta}(\mathbf{k})$, representing the x, y components of the mode. These vectors are given by $\hat{\mathbf{e}}^L(\mathbf{k}) = (\cos \phi_k, \sin \phi_k)$ and $\hat{\mathbf{e}}^T(\mathbf{k}) = (\sin \phi_k, -\cos \phi_k)$ for a pure longitudinal and transverse mode, but generally speaking, the LA and TA phonon modes are not entirely longitudinal or transverse, $\hat{\mathbf{e}}^L(\mathbf{k}) \nparallel \mathbf{k}$ and $\hat{\mathbf{e}}^T(\mathbf{k}) \nperp \mathbf{k}$, unless $\mathbf{k} = (k_x, k_y)$ are along the high symmetry directions, e.g., $(1, 0)$, $(1, 1)$, $(0, 1)$. One special case is that $a_1 = 2a_2$, when $\omega_p^{L/T}(\mathbf{k})$ are isotropic and LA and TA phonons are pure longitudinal and transverse in any direction in long wavelength limit. We show the magnon and three phonon dispersions in Fig. 2. Without magnon-phonon coupling, the gapped magnon band crosses with each of the gapless phonon band at a ring of momentum satisfies $\omega_m(\mathbf{k}) = \omega_p^i(\mathbf{k})$. We do not include the second possible band crossing at larger momentum [24] as they are of much higher energy, and therefore less significant for transport at sufficiently low temperature.

C. Magnetoelastic Coupling

The magnetoelastic coupling is generally modeled by the following energy density [26], which takes into account of the interaction between the magnetization and lattice deformation due to strain.

$$\begin{aligned} \epsilon_{\text{mp}} &= \kappa_1 (S_x^2 e_{xx} + S_y^2 e_{yy} + S_z^2 e_{zz}) \\ &\quad + \kappa_2 (S_x S_y e_{xy} + S_x S_z e_{xz} + S_y S_z e_{yz}), \end{aligned} \quad (11)$$

where $e_{mn} = \partial u^m / \partial n + \partial u^n / \partial m$.

We can use the three-dimensional rotation matrix \mathcal{R} that transforms the z axis to the equilibrium spin direction \mathbf{n}_0 : $\mathbf{n}_0 = \mathcal{R}\mathbf{n}'_0$, with $\mathbf{n}'_0 = \hat{z}$ and $\mathbf{n}_0 = (\sin \theta, 0, \cos \theta)$. Using the rotational transformation,

$$\begin{pmatrix} S_x \\ S_y \\ S_z \end{pmatrix} = \begin{pmatrix} \cos \theta & 0 & \sin \theta \\ 0 & 1 & 0 \\ -\sin \theta & 0 & \cos \theta \end{pmatrix} \begin{pmatrix} S_{x'} \\ S_{y'} \\ S_{z'} \end{pmatrix}, \quad (12)$$

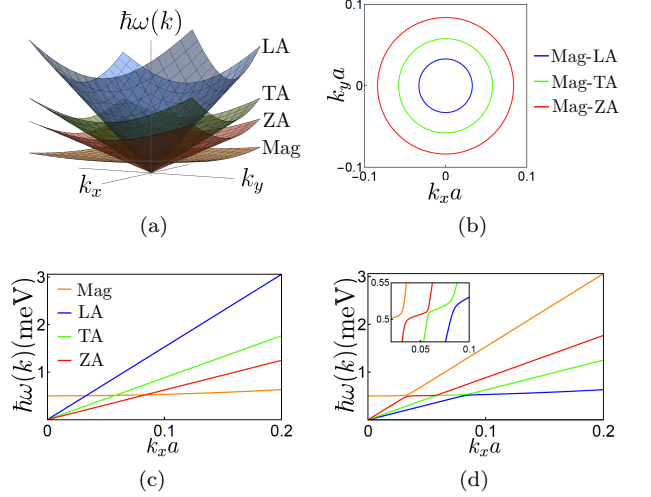


FIG. 2: Dispersion relation of excitation bands with magnetic field tilt angle $\theta = \pi/8$ and parameters used are given in the main text of Sec. III. (a) Dispersion of ZA, LA, TA phonons and magnons, denoted by Mag, without magnetoelastic coupling. (b) Contour plot of the rings of momentum that magnons cross with LA, TA and ZA phonons. (c) Dispersion in k_x direction without magnetoelastic coupling. (d) Hybridization of magnons and ZA, LA, TA phonons in k_x direction in the presence of magnetoelastic coupling. Inset is a zoom-in of magnons and phonons crossing.

we obtain the magnetoelastic energy density in linear order of the magnon amplitude, $S_{x'}$ and $S_{y'}$,

$$\begin{aligned} \epsilon_{\text{mp}} &= \kappa_1 \sin 2\theta S_{x'} S_{z'} e_{xx} + \kappa_2 \sin \theta S_{y'} S_{z'} e_{xy} \\ &\quad + \kappa_2 \cos 2\theta S_{x'} S_{z'} e_{xz} + \kappa_2 \cos \theta S_{y'} S_{z'} e_{yz} \end{aligned} \quad (13)$$

In terms of the magnon and phonon operator introduced earlier in Eq. (3) and Eq. (7), the magnetoelastic coupling term can be recast into particle-number-conserving terms, $a^\dagger b, ab^\dagger$, and particle-number-nonconserving terms, $a^\dagger b^\dagger, ab$. We follow Ref. [24] by neglecting the particle-number-nonconserving terms because the effect of those on band structure is of quadratic order in the magnetoelastic coupling and thus is much smaller than the effect of the particle-number-conserving terms.

The particle-number-conserving Hamiltonian is then given by

$$H \approx \sum_{\mathbf{k}} (a_{\mathbf{k}}^\dagger, b_{\mathbf{k}}^{L\dagger}, b_{\mathbf{k}}^{T\dagger}, b_{\mathbf{k}}^{Z\dagger}) \mathcal{H}_{\mathbf{k}} \begin{pmatrix} a_{\mathbf{k}} \\ b_{\mathbf{k}}^L \\ b_{\mathbf{k}}^T \\ b_{\mathbf{k}}^Z \end{pmatrix}, \quad (14)$$

with

$$\mathcal{H}_{\mathbf{k}} = \begin{pmatrix} \hbar\omega_m(\mathbf{k}) & M_L & M_T & M_Z \\ M_L^* & \hbar\omega_p^L(\mathbf{k}) & 0 & 0 \\ M_T^* & 0 & \hbar\omega_p^T(\mathbf{k}) & 0 \\ M_Z^* & 0 & 0 & \hbar\omega_p^Z(\mathbf{k}) \end{pmatrix}, \quad (15)$$

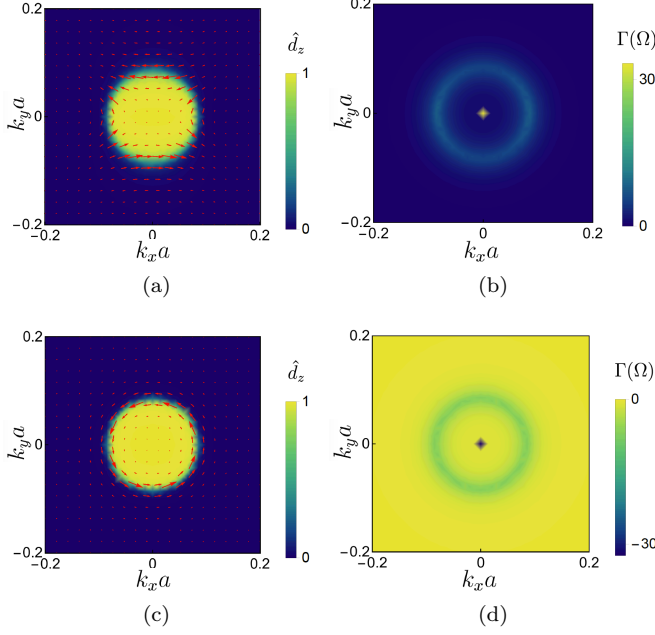


FIG. 3: The Berry curvatures of the upper band in log-scale $\Gamma(\Omega) = \text{sign}(\Omega) \log(1 + |\Omega|)$ (right) and schematic illustration of $\hat{\mathbf{d}}(\mathbf{k})$ (left) from magnon and ZA phonon coupling. The in-plane components of the $\hat{\mathbf{d}}$ vector, (\hat{d}_x, \hat{d}_y) , are shown as arrows. (a, b) Magnetic field with tilt angle $\theta = \pi/8$. (c, d) Magnetic field with tilt angle $\theta = 3\pi/8$.

where

$$\begin{aligned} M_L &= \tilde{\kappa}_L \left[\frac{\kappa_1}{\kappa_2} 2 \sin 2\theta e_x^L i k_x - \sin \theta e_x^L k_y - \sin \theta e_y^L k_x \right], \\ M_T &= \tilde{\kappa}_T \left[\frac{\kappa_1}{\kappa_2} 2 \sin 2\theta e_x^T i k_x - \sin \theta e_x^T k_y - \sin \theta e_y^T k_x \right], \\ M_Z &= \tilde{\kappa}_Z (\cos 2\theta i k_x - \cos \theta k_y), \end{aligned} \quad (16)$$

and $\tilde{\kappa}_i = \frac{\kappa_2}{2} S \sqrt{\frac{\hbar S}{M \omega_p^i(\mathbf{k})}}$.

In the case of $a_1 = 2a_2$ when LA phonon is pure longitudinal and TA phonon is pure transverse,

$$\begin{aligned} M_L &= \tilde{\kappa}_L \left(\frac{\kappa_1}{\kappa_2} 2 \sin 2\theta \cos^2 \phi_k i - \sin \theta \sin 2\phi_k \right) k, \\ M_T &= \tilde{\kappa}_T \left(\frac{\kappa_1}{\kappa_2} \sin 2\theta \sin 2\phi_k i + \sin \theta \cos 2\phi_k \right) k, \\ M_Z &= \tilde{\kappa}_Z (\cos 2\theta \cos \phi_k i - \cos \theta \sin \phi_k) k. \end{aligned} \quad (17)$$

The band structure of magnon-phonon hybrid system is obtained by diagonalizing Eq. (15). Without magnon-phonon coupling, magnon band crosses with ZA, LA, TA phonon band and the excitations are not hybridized. With the presence of magnon-phonon couplings, bands open up the gaps at the bands crossing rings and form hybridized excitations, namely magnon-polarons, which induces the nontrivial topological properties of the bands,

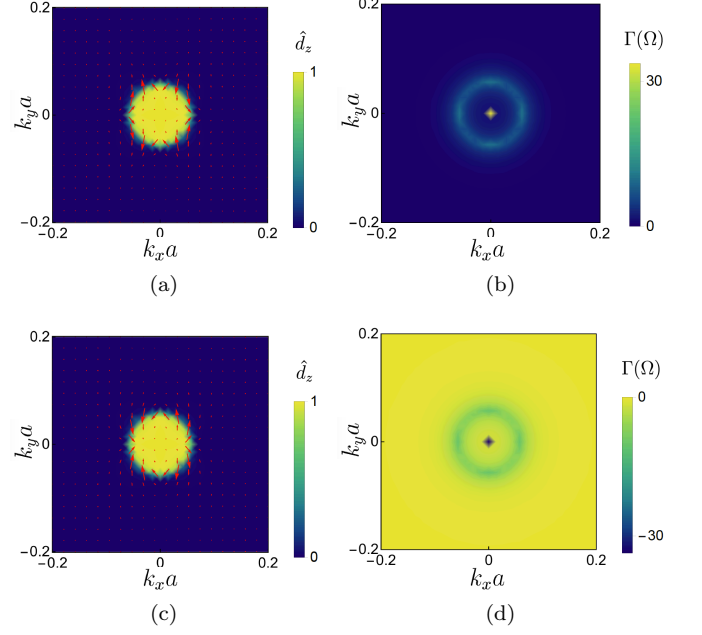


FIG. 4: The Berry curvatures of the upper band in log-scale $\Gamma(\Omega) = \text{sign}(\Omega) \log(1 + |\Omega|)$ (right) and schematic illustration of $\mathbf{d}(\mathbf{k})$ (left) from magnon and TA phonon coupling, the in-plane components of the $\hat{\mathbf{d}}$ vector, (\hat{d}_x, \hat{d}_y) are shown as arrows. (a, b) Magnetic field with tilt angle $\theta = \pi/4$. (c, d) Magnetic field with tilt angle $\theta = 3\pi/4$.

characterized by the Berry curvature. See Fig. 2(d) for the hybridized bands plot.

III. TOPOLOGICAL PROPERTIES

The rigorous calculation of band structure and Chern number can be done with SU(4) formalism [31]. For weak coupling [25], the Berry curvature concentrates in the vicinity of the avoided crossing ring, while the three rings of momentum satisfying $\omega_m(\mathbf{k}) = \omega_p^i(\mathbf{k})$ are relatively separated from each other. We can use the familiar two-band theory of topological insulator [9, 32] to understand the band topology by focusing on each pair of magnon and phonon bands.

We can write the Bloch Hamiltonian, Eq. (15) in the following form near each band crossing:

$$\mathcal{H}_k = \begin{pmatrix} \mathcal{H}_{2 \times 2}^i(\mathbf{k}) & 0 & 0 \\ 0 & \hbar \omega_p^j(\mathbf{k}) & 0 \\ 0 & 0 & \hbar \omega_p^k(\mathbf{k}) \end{pmatrix} + \mathcal{V}_k, \quad (18)$$

where \mathcal{V}_k is a perturbation term that does not participate in opening the gap between the two bands $(\varepsilon_m, \varepsilon_p^i)$, and $\mathcal{H}_{2 \times 2}^i(\mathbf{k})$ can be written into the form of

$$\mathcal{H}^i(\mathbf{k}) = \frac{1}{2} \hbar (\omega_m + \omega_p^i) I + \mathbf{d}^i(\mathbf{k}) \cdot \boldsymbol{\sigma}, \quad (19)$$

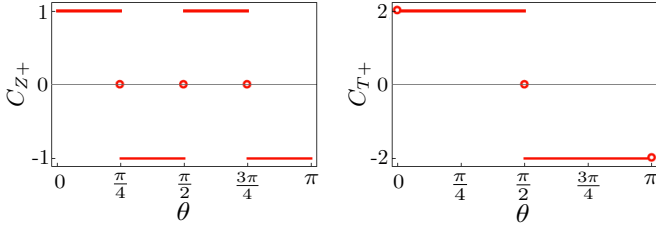


FIG. 5: Dependence of the Chern number of upper branch $C_{i,+}$ on tilt angle θ (a) for the hybridization of magnons and ZA phonons and (b) for the hybridization of magnons and TA phonons. $|C_{Z,+}| = 1$ and its sign changes at $\theta = \pi/4, \pi/2$ and $3\pi/4$. $|C_{T,+}| = 2$ and its sign changes at $\theta = \pi/2$.

with $\sigma = (\sigma_x, \sigma_y, \sigma_z)$ are Pauli matrices and $\mathbf{d}^i(\mathbf{k})$ for each band crossing are

$$\begin{aligned} \mathbf{d}^Z(\mathbf{k}) &= [-\tilde{\kappa}_Z \cos \theta \sin \phi_k k, -\tilde{\kappa}_Z \cos 2\theta \cos \phi_k k, \\ &\quad \frac{1}{2} \hbar(\omega_m - \omega_p^Z)] \\ \mathbf{d}^L(\mathbf{k}) &= [-\tilde{\kappa}_L \sin \theta \sin 2\phi_k k, -\tilde{\kappa}_L \frac{\kappa_1}{\kappa_2} 2 \sin 2\theta \cos^2 \phi_k k, \\ &\quad \frac{1}{2} \hbar(\omega_m - \omega_p^L)], \\ \mathbf{d}^T(\mathbf{k}) &= [\tilde{\kappa}_T \sin \theta \cos 2\phi_k k, -\tilde{\kappa}_T \frac{\kappa_1}{\kappa_2} \sin 2\theta \sin 2\phi_k k, \\ &\quad \frac{1}{2} \hbar(\omega_m - \omega_p^T)]. \end{aligned} \quad (20)$$

In terms of the normalized vector $\hat{\mathbf{d}} = \mathbf{d}/|\mathbf{d}|$, the Berry curvature is written explicitly as

$$\Omega_{\pm}^i(\mathbf{k}) = \mp \frac{1}{2} \hat{\mathbf{d}}^i(\mathbf{k}) \cdot \left(\frac{\partial \hat{\mathbf{d}}^i(\mathbf{k})}{\partial k_x} \times \frac{\partial \hat{\mathbf{d}}^i(\mathbf{k})}{\partial k_y} \right), \quad (21)$$

where $+$ and $-$ are for upper and lower bands, respectively. The corresponding expression for Chern number is given by [32–34]

$$C_{i,\pm} = \frac{1}{2\pi} \int d^2k \Omega_{\pm}^i(\mathbf{k}), \quad (22)$$

which is the skyrmion number of the $\hat{\mathbf{d}}$ vector [32], counting how many times $\hat{\mathbf{d}}$ wraps the unit sphere in the Brillouin zone.

We note that the magnon and LA phonon coupling always vanishes in k_y direction. This can be understood from Eq. (13). As we set the magnetic field in x-z plane, there is no term with $e_{yy} = \partial u_y / \partial y$. This means LA phonons at k_y direction does not couple to magnons and the two hybridized bands are touching at $(0, \pm k_y)$. The Berry curvatures at the touching points are not well defined. Similar phenomena has also been found in Weyl semimetal and such points are called Weyl points [35]. The corresponding Chern number from magnon and ZA phonon coupling is $|C_Z| = 1$ and one for magnon and TA

phonon coupling is $|C_T| = 2$, which can be easily understood by the dependence of polar angle ϕ_k in Eq. (20). Prefactor of d_x^Z and d_y^T change sign across $\theta = \pi/2$, and prefactor of d_y^Z changes sign across $\theta = \pi/4$ and $3\pi/4$. Across each of these angles, $\hat{\mathbf{d}}$ changes its winding direction, and therefore there is a topological transition as well. See Fig. 5 for the dependence of Chern number on magnetic field tilt angle θ from 0 to π . When $\theta = \pi/4$ or $3\pi/4$, the magnon and ZA phonon coupling vanishes in the k_x direction. When $\theta = \pi/2$, the magnon and ZA phonon coupling vanishes in the k_y direction and the magnon and TA phonon coupling vanishes in the direction of $\phi_k = n\pi/4$ with odd integer n . The Berry curvatures are not well defined at the band touching points at these critical angles. When $\theta = 0$ and π , there is no coupling between magnons and LA, TA phonons at any momentum. Hybridization only occurs between magnons and ZA phonons as previously reported [24].

The above discussion about band touching and topological transition holds even if $a_1 \neq 2a_2$ since the phonon modes are always longitudinal or transverse in the direction of $\phi_k = n\pi/4$ with integer n . The effect can be shown by replacing ϕ_k in $\hat{\mathbf{e}}^{L/T}(\phi_k)$ with function $\psi(\phi_k)$, where $\psi(\phi_k)$ is a monotonically increasing function of ϕ_k and satisfies $\psi(\phi_k) = \phi_k$ at $\phi_k = n\pi/4$.

We show the change of the Berry curvatures and the topological properties for magnon and ZA phonon coupling in Fig. 3 and magnon and TA phonon coupling in Fig. 4. For calculation, we used the parameters of the monolayer ferromagnet CrI₃ in Refs. [21, 36–38] ($J=2.2$ meV, $S=3/2$, $Mc^2=5 \times 10^{10}$ eV). The force constant is taken $a_1=2 \times 10^5$ meV/nm², $a_2=10^5$ meV/nm², $a_3=5 \times 10^4$ meV/nm²; the coupling strengths are taken $\kappa_1=10$ meV/nm and $\kappa_2=5$ meV/nm. The external magnetic field is taken $B=0.5$ meV. We found the dominant contribution of the Berry curvature comes from vicinity of the ring where two bands cross and it changes sign across the critical angles as shown in Fig. 3(b, d) and Fig. 4(b, d). Note that there is singularity of the Berry curvature near $k = 0$. This originates from the $1/\sqrt{\omega_{\mathbf{k}}}$ dependence of $\tilde{\kappa}$ in $\mathbf{d}(\mathbf{k})$. We verified that its contribution to the Chern number and thermal Hall conductivity is negligible despite the divergence. In Fig. 3(a, c), we found that the skyrmion number of $\hat{\mathbf{d}}$ vector at magnon and ZA phonon crossing corresponds to $C_+ = 1$ at $\theta = \pi/8$ and corresponds to $C_+ = -1$ at $\theta = 3\pi/8$. In Fig. 4(a, c), we found that the skyrmion number of $\hat{\mathbf{d}}$ vector at magnon and TA phonon crossing corresponds to $C_+ = 2$ at $\theta = \pi/4$ and it corresponds to $C_+ = -2$ at $\theta = 3\pi/4$.

IV. THERMAL HALL CONDUCTIVITY

The finite Berry curvatures of magnon-phonon hybrid excitations give rise to the intrinsic thermal Hall effect as shown below. The semiclassical equations of motion for

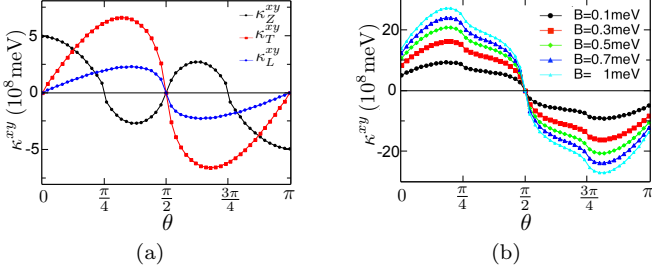


FIG. 6: (a) The contributions κ_Z^{xy} , κ_T^{xy} and κ_L^{xy} to the thermal Hall conductivities from magnon-ZA phonon coupling, magnon-LA phonon coupling, and magnon-TA phonon coupling, respectively. Parameter used are $T=10$ K and $B=0.1$ meV. (b) Dependence of the total thermal Hall conductivity κ^{xy} on the tilt angle for several different magnetic fields at $T=10$ K.

the wave packet of magnon-polarons are given by [39, 40]

$$\dot{\mathbf{r}} = \frac{1}{\hbar} \frac{\partial E_n(\mathbf{k})}{\partial \mathbf{k}} - \dot{\mathbf{k}} \times \Omega_n(\mathbf{k}), \quad \hbar \dot{\mathbf{k}} = -\nabla U(\mathbf{r}), \quad (23)$$

where $U(r)$ is the potential acting on the wave packet which can be regarded as a confining potential of the bosonic excitation.

The Berry-curvature-induced thermal Hall conductivity is given by [12, 13]

$$\kappa^{xy} = -\frac{k_B^2 T}{\hbar V} \sum_{n, \mathbf{k}} c_2(\rho_{n, \mathbf{k}}) \Omega_n(\mathbf{k}), \quad (24)$$

where $c_2(\rho) = (1 + \rho) \ln^2[(1 + \rho)/\rho] - \ln^2 \rho - 2\text{Li}_2(-\rho)$, $\rho_{n, \mathbf{k}} = [e^{E_n(\mathbf{k})/k_B T} - 1]^{-1}$ is Bose-Einstein distribution function with a zero chemical potential, k_B is the Boltzmann constant, T is the temperature, and $\text{Li}_2(z)$ is the polylogarithm function.

In Fig. 6(a), we show the dependence of thermal Hall conductivity on the magnetic field tilt angle from contribution of magnon with ZA, LA, TA phonon coupling separately at $B = 0.1$ meV. At $\theta = 0$, there is no contribution from LA and TA phonon because there is no Berry curvature from them. Across $\theta = \pi/4$, the contribution of ZA phonon becomes negative because the Berry curvature change sign at this angle. At $\theta = \pi/2$, when the ground state spin direction is in-plane, all the contributions vanish and the thermal Hall conductivity becomes zero as expected from the general symmetry grounds as follows. The thermal Hall conductivity is odd under time reversal: $\kappa^{xy}(\theta) = -\kappa^{xy}(\pi + \theta)$. Our system respects the two-fold rotational symmetry: $\kappa^{xy}(\theta) = \kappa^{xy}(2\pi - \theta)$. Then, it follows $\kappa^{xy}(\theta) = -\kappa^{xy}(\pi - \theta)$. In particular, we have $\kappa^{xy}(\pi/2) = 0$, implying the absence of the thermal Hall effect for the in-plane magnetic field. In summary, the thermal Hall conductivity starts from a finite positive value at $\theta = 0$. It starts to increase as the angle increases

and reaches the maximum, then decreases to the negative minimum by passing zero at $\theta = \pi/2$. Eventually, it increases to a negative value at $\theta = \pi$ as shown in Fig. 6(b).

V. DISCUSSION

In this paper, we studied topological properties of magnon-polarons in a square lattice ferromagnet with Kittel's magnetoelastic interaction subjected to a magnetic field in an arbitrary direction. In our model, the magnons couples with longitudinal and transverse in-plane phonons as well as out-of-plane phonons. We investigated the topological structure of the magnon-polaron bands by mapping our model to the well-known two-band model of topological insulator near each band crossing point. The Berry curvature and the Chern number corresponding to three hybridizations are found to differ as follows. First, magnons and out-of-plane phonons coupling gives rise to a Chern number $|C|=1$, which changes sign at $\theta = \pi/4, \pi/2$ and $3\pi/4$. Secondly, magnons and transverse in-plane phonons coupling gives rise to a Chern number $|C|=2$, which changes sign at $\theta = \pi/2$. Thirdly, the hybridization of magnons and longitudinal in-plane phonons does not possess the well-defined Chern number since there are two points in the momentum space where the gap is not opened up. We also calculated the dependence of thermal Hall conductivity based on our model as an experimental probe. The unique behavior of thermal Hall conductivity as a function of the field direction reflects the contributions from in-plane and out-of plane phonons and can be used to probe the topological tunability of the magnon-polaron bands.

Kittel's magnetoelastic interaction originates from the magnetic anisotropy, which is ubiquitous in ferromagnetic thin film structure [41], but the effect of magnetoelastic coupling on magnetic dynamics is still largely unknown. In our model, we used a Hamiltonian that is bilinear in the magnon and phonon operator, which result in the hybridization of magnon and phonon mode, by neglecting higher-order terms. If magnetoelastic interaction is sufficiently strong, the band will be strongly renormalized [42] and may require the inclusion of the higher-order terms. The physics of strong magnetoelastic interaction could be more pronounced in two dimensional magnets with weak mechanical stability [43, 44], which will be pursued in the future.

ACKNOWLEDGMENTS

The authors appreciate the useful discussions with Kyung-Jin Lee, Gyungchoon Go, and Shu Zhang. This work is supported by the University of Missouri. S.K.K. acknowledges Young Investigator Grant (YIG) from Korean-American Scientists and Engineers Association (KSEA).

-
- [1] K. v. Klitzing, G. Dorda, and M. Pepper, “New method for high-accuracy determination of the fine-structure constant based on quantized hall resistance,” *Phys. Rev. Lett.* **45**, 494–497 (1980).
- [2] R. B. Laughlin, “Quantized hall conductivity in two dimensions,” *Phys. Rev. B* **23**, 5632–5633 (1981).
- [3] F. D. M. Haldane, “Model for a quantum hall effect without landau levels: Condensed-matter realization of the “parity anomaly,”” *Phys. Rev. Lett.* **61**, 2015–2018 (1988).
- [4] Michael Victor Berry, “Quantal phase factors accompanying adiabatic changes,” *Proc. Royal Soc. Lond. A* **392**, 45–57 (1984).
- [5] Shigeki Onoda, Naoyuki Sugimoto, and Naoto Nagaosa, “Intrinsic versus extrinsic anomalous hall effect in ferromagnets,” *Phys. Rev. Lett.* **97**, 126602 (2006).
- [6] N. A. Sinitsyn, A. H. MacDonald, T. Jungwirth, V. K. Dugaev, and Jairo Sinova, “Anomalous hall effect in a two-dimensional dirac band: The link between the kubo-streda formula and the semiclassical boltzmann equation approach,” *Phys. Rev. B* **75**, 045315 (2007).
- [7] Shuichi Murakami, Naoto Nagaosa, and Shou-Cheng Zhang, “Dissipationless quantum spin current at room temperature,” *Science* **301**, 1348–1351 (2003).
- [8] C. L. Kane and E. J. Mele, “ Z_2 topological order and the quantum spin hall effect,” *Phys. Rev. Lett.* **95**, 146802 (2005).
- [9] B. Andrei Bernevig, Taylor L. Hughes, and Shou-Cheng Zhang, “Quantum spin hall effect and topological phase transition in hgte quantum wells,” *Science* **314**, 1757–1761 (2006).
- [10] Hosho Katsura, Naoto Nagaosa, and Patrick A. Lee, “Theory of the thermal hall effect in quantum magnets,” *Phys. Rev. Lett.* **104**, 066403 (2010).
- [11] Y. Onose, T. Ideue, H. Katsura, Y. Shiomi, N. Nagaosa, and Y. Tokura, “Observation of the magnon hall effect,” *Science* **329**, 297–299 (2010).
- [12] Ryo Matsumoto and Shuichi Murakami, “Theoretical prediction of a rotating magnon wave packet in ferromagnets,” *Phys. Rev. Lett.* **106**, 197202 (2011).
- [13] Ryo Matsumoto and Shuichi Murakami, “Rotational motion of magnons and the thermal hall effect,” *Phys. Rev. B* **84**, 184406 (2011).
- [14] Ryuichi Shindou, Ryo Matsumoto, Shuichi Murakami, and Jun-ichiro Ohe, “Topological chiral magnonic edge mode in a magnonic crystal,” *Phys. Rev. B* **87**, 174427 (2013).
- [15] Lifa Zhang, Jie Ren, Jian-Sheng Wang, and Baowen Li, “Topological nature of the phonon hall effect,” *Phys. Rev. Lett.* **105**, 225901 (2010).
- [16] Pai Wang, Ling Lu, and Katia Bertoldi, “Topological phononic crystals with one-way elastic edge waves,” *Phys. Rev. Lett.* **115**, 104302 (2015).
- [17] S. Hossein Mousavi, Alexander B. Khanikaev, and Zheng Wang, “Topologically protected elastic waves in phononic metamaterials,” *Nat. Commun.* **6**, 8682 (2015).
- [18] Naoki Ogawa, Wataru Koshibae, Aron Jonathan Beekman, Naoto Nagaosa, Masashi Kubota, Masashi Kawasaki, and Yoshinori Tokura, “Photodrive of magnetic bubbles via magnetoelastic waves,” *Proc. Natl. Acad. Sci. U.S.A* **112**, 8977–8981 (2015).
- [19] Takashi Kikkawa, Ka Shen, Benedetta Flebus, Rembert A. Duine, Ken-ichi Uchida, Zhiyong Qiu, Gerrit E. W. Bauer, and Eiji Saitoh, “Magnon polarons in the spin seebeck effect,” *Phys. Rev. Lett.* **117**, 207203 (2016).
- [20] Ryuji Takahashi and Naoto Nagaosa, “Berry curvature in magnon-phonon hybrid systems,” *Phys. Rev. Lett.* **117**, 217205 (2016).
- [21] Xiaou Zhang, Yinhan Zhang, Satoshi Okamoto, and Di Xiao, “Thermal hall effect induced by magnon-phonon interactions,” *arXiv:1903.07702* (2019).
- [22] Sungjoon Park and Bohm-Jung Yang, “Topological magnetoelastic excitations in noncollinear antiferromagnets,” *Phys. Rev. B* **99**, 174435 (2019).
- [23] Sungjoon Park, Naoto Nagaosa, and Bohm-Jung Yang, “Thermal hall effect, spin nerst effect, and spin density induced by thermal gradient in collinear ferrimagnets from magnon-phonon interaction,” *arXiv:1910.07206* (2019).
- [24] Gyungchoon Go, Se Kwon Kim, and Kyung-Jin Lee, “Topological magnon-phonon hybrid excitations in two-dimensional ferromagnets with tunable chern numbers,” *arXiv:1907.02224* (2019).
- [25] Shu Zhang, Gyungchoon Go, Kyung-Jin Lee, and Se Kwon Kim, “ $Su(3)$ topology of magnon-phonon hybridization in 2d antiferromagnets,” *arXiv:1909.08031* (2019).
- [26] C. Kittel, “Interaction of spin waves and ultrasonic waves in ferromagnetic crystals,” *Phys. Rev.* **110**, 836–841 (1958).
- [27] Charles Kittel, *Introduction to solid state physics*, Vol. 8 (Wiley New York, 1976).
- [28] M. Mohr, J. Maultzsch, E. Dobardvzić, S. Reich, I. Milovsević, M. Damnjanović, A. Bosak, M. Krisch, and C. Thomsen, “Phonon dispersion of graphite by inelastic x-ray scattering,” *Phys. Rev. B* **76**, 035439 (2007).
- [29] A. Molina-Sánchez and L. Wirtz, “Phonons in single-layer and few-layer mo_2 and ws_2 ,” *Phys. Rev. B* **84**, 155413 (2011).
- [30] Denis L Nika and Alexander A Balandin, “Two-dimensional phonon transport in graphene,” *J. Phys. Condens. Matter* **24**, 233203 (2012).
- [31] Ryan Barnett, G. R. Boyd, and Victor Galitski, “ $Su(3)$ spin-orbit coupling in systems of ultracold atoms,” *Phys. Rev. Lett.* **109**, 235308 (2012).
- [32] Xiao-Liang Qi, Taylor L. Hughes, and Shou-Cheng Zhang, “Topological field theory of time-reversal invariant insulators,” *Phys. Rev. B* **78**, 195424 (2008).
- [33] Xiao-Liang Qi, Yong-Shi Wu, and Shou-Cheng Zhang, “Topological quantization of the spin hall effect in two-dimensional paramagnetic semiconductors,” *Phys. Rev. B* **74**, 085308 (2006).
- [34] G. E. Volovik, “An analog of the quantum hall effect in a superfluid 3he film,” *J. Exp. Theor. Phys.* **67**, 1804–1811 (1988).
- [35] N. P. Armitage, E. J. Mele, and Ashvin Vishwanath, “Weyl and dirac semimetals in three-dimensional solids,” *Rev. Mod. Phys.* **90**, 015001 (2018).
- [36] Wei-Bing Zhang, Qian Qu, Peng Zhu, and Chi-Hang Lam, “Robust intrinsic ferromagnetism and half semiconductivity in stable two-dimensional single-layer chromium trihalides,” *J. Mater. Chem. C* **3**, 12457–12468 (2015).

- (2015).
- [37] Bevin Huang, Genevieve Clark, Efrén Navarro-Moratalla, Dahlia R. Klein, Ran Cheng, Kyle L. Seyler, Ding Zhong, Emma Schmidgall, Michael A. McGuire, David H. Cobden, Wang Yao, Di Xiao, Pablo Jarillo-Herrero, and Xiaodong Xu, “Layer-dependent ferromagnetism in a van der waals crystal down to the monolayer limit,” *Nature* **546**, 270 EP – (2017).
 - [38] J L Lado and J Fernández-Rossier, “On the origin of magnetic anisotropy in two dimensional CrI₃,” *2D Materials* **4**, 035002 (2017).
 - [39] Di Xiao, Ming-Che Chang, and Qian Niu, “Berry phase effects on electronic properties,” *Rev. Mod. Phys.* **82**, 1959–2007 (2010).
 - [40] Ganesh Sundaram and Qian Niu, “Wave-packet dynamics in slowly perturbed crystals: Gradient corrections and berry-phase effects,” *Phys. Rev. B* **59**, 14915–14925 (1999).
 - [41] B. Dieny and M. Chshiev, “Perpendicular magnetic anisotropy at transition metal/oxide interfaces and applications,” *Rev. Mod. Phys.* **89**, 025008 (2017).
 - [42] Nobuo Furukawa, “Magnon linewidth broadening due to magnon-phonon interactions in colossal magnetoresistance manganites,” *J. Phys. Soc. Jpn.* **68**, 2522–2525 (1999).
 - [43] L. M. Woods, “Magnon-phonon effects in ferromagnetic manganites,” *Phys. Rev. B* **65**, 014409 (2001).
 - [44] Kenneth S. Burch, David Mandrus, and Je-Geun Park, “Magnetism in two-dimensional van der waals materials,” *Nature* **563**, 47–52 (2018).